Electronic Supplementary Material (ESI) for RSC Advances.

Supporting information

Table S1 Selected hydrogen bonds lengths [Å] and angles [°] for **1-5**.

Donor-H···Acceptor	D-H	H···A	D···A	D-H···A
1				
N4-H4A···O4	0.92	2.09	3.0053	171
O5-H5A···O11	0.85	1.87	2.7130	169
O5-H5B···N6	0.85	1.99	2.8438	178
O6-H6A···O8	0.85	1.91	2.7225	160
N8-H8A···O3	0.92	2.18	3.0774	166
2				
O1-H1A···F1	0.85	1.84	2.669(3)	164
O5-H1B···F5	0.85	1.80	2.649(2)	172
O2-H2A···F3	0.85	1.82	2.667(3)	174
O2-H2B···F3	0.85	1.83	2.673(3)	168
3				
O5-H5A···N2	0.82	2.04	2.8554	171
O5-H5B···O7	0.79	1.95	2.7375	175
N8-H8A···O3B	0.92	2.06	2.9741	170
N8-H8B···N6	0.92	2.22	3.1204	166
4				
N4-H4A···N2	0.90	2.40	3.267(3)	160
N4-H4B···O4	0.90	2.15	3.043(3)	170
N8-H8B···O1	0.90	2.11	2.998(3)	169
5				
N4-H4A···O8	0.92	2.15	2.9864	151
N4-H4B···O7	0.92	2.38	3.2194	152
N8-H8A···O3	0.92	2.23	3.0835	155

Table S2. Selected Bond Lengths [Å] and Angles [º] for Complexes **1**-**5**[a].

		1			
Cd(1)-N(7)	2.296(3)	Cd(1)-N(3)	2.301(3)	Cd(1)-O(5)	2.313(2)
Cd(1)-O(6)	2.361(2)	Cd(1)-N(4)	2.374(2)	Cd(1)-N(8A)	2.395(3)
N(7)-Cd(1)-N(3)	92.24(9)	N(7)-Cd(1)-O(5)	87.22(8)	N(3)-Cd(1)-O(5)	89.63(9)
N(7)-Cd(1)-O(6)	90.30(9)	N(3)-Cd(1)-O(6)	173.34(8)	O(5)-Cd(1)-O(6)	84.35(8)
N(7)-Cd(1)-N(4)	91.75(9)	N(3)-Cd(1)-N(4)	96.08(9)	O(5)-Cd(1)-N(4)	174.24(9)
O(6)-Cd(1)-N(4)	89.99(9)	N(7)-Cd(1)-N(8A)	175.13(9)	N(3)-Cd(1)-N(8A)	90.38(9)
O(5)-Cd(1)-N(8A)	88.69(9)	O(6)-Cd(1)-N(8)	86.66(9)	N(4)#1-Cd(1)-N(8A)	92.06(9)
		2			
Cd(1)-O(1)	2.282(2)	Cd(1)-O(1A)	2.282(2)	Cd(1)-N(7A)	2.329(2)
Cd(1)-N(7)	2.329(2)	Cd(1)-N(4)	2.376(2)	Cd(1)-N(4A)	2.376(2)
Cd(2)-N(3)	2.317(2)	Cd(2)-N(3)	2.317(2)	Cd(2)-O(2)	2.321(2)
Cd(2)-O(2B)	2.321(2)	Cd(2)-N(8)	2.374(2)	Cd(2)-N(8B)	2.374(2)
O(1)-Cd(1)-O(1A)	180.0	O(1)-Cd(1)-N(7A)	86.84(8)	O(1)-Cd(1)-N(7A)	93.16(8)
O(1)-Cd(1)-N(4)	91.24(8)	O(1)-Cd(1)-N(4A)	88.77(8)	N(4)-Cd(1)-N(4A)	180.00(10)
N(3)-Cd(2)-O(2)	87.30(8)	N(3)-Cd(2)-N(8)	93.96(8)	O(2)-Cd(2)-N(8)	82.23(8)
N(3)-Cd(2)-N(8B)	86.04(8)	N(8)-Cd(2)-N(8B)	179.999(1)		
		3			
Cd(1)-N(7)	2.309(2)	Cd(1)-N(3)	2.304(3)	Cd(1)-O(5)	2.314(2)
Cd(1)-O(6)	2.358(2)	Cd(1)-N(4)	2.401(3)	Cd(1)-N(8A)	2.385(3)
N(3)-Cd(1)-N(7)	92.90(10)	N(3)-Cd(1)-O(5)	87.28(9)	N(7)-Cd(1)-O(5)	89.69(9)
N(3)-Cd(1)-O(6)	89.82(10)	N(7)-Cd(1)-O(6)	173.16(10)	O(5)-Cd(1)-O(6)	84.17(10)
N(3)-Cd(1)-N(8A)	91.56(9)	N(7)-Cd(1)-N(8A)	96.38(9)	O(5)-Cd(1)-N(8A)	173.88(8)
O(6)-Cd(1)-N(8A)	89.82(10)	N(3)-Cd(1)-N(4)	175.15(9)	N(7)-Cd(1)-N(4)	90.19(9)
O(5)-Cd(1)-N(4)	89.00(10)	O(6)-Cd(1)-N(4)	86.70(10)	N(8A)-Cd(1)-N(4)	91.82(9)
		4			
Cd(1)-N(9A)	2.290(2)	Cd(1)-N(7)	2.304(2)	Cd(1)-N(3)	2.319(2)
Cd(1)-N(4A)#2	2.419(2)	Cd(1)-N(8A)	2.458(2)	Cd(1)-S(1)	2.8490(8)

N(9A)-Cd(1)-N(7)	100.05(8)	N(9A)-Cd(1)-N(3)	163.37(8)	N(7)-Cd(1)-N(3)	92.84(8)
N(3)-Cd(1)-N(4A)	94.57(7)	N(7)-Cd(1)-N(8A)	175.50(7)	N(3)-Cd(1)-N(8A)	85.05(8)
N(7)-Cd(1)-S(1)	79.94(5)	N(3)-Cd(1)-S(1)	86.37(5)	N(8A)-Cd(1)-S(1)	103.86(5)
		5			
Ag(1)-N(6A)	2.247(3)	Ag(1)-N(8)	2.270(3)	Ag(1)-N(4)	2.426(3)
Ag(2)-N(3A)	2.143(3)	Ag(2)-N(3)	2.143(3)	Ag(3)-N(7)	2.153(3)
Ag(3)-N(7A)	2.153(3)	N(6A)-Ag(1)-N(8)	141.92(10)	N(6A)-Ag(1)-N(4)	91.42(10)
N(8)-Ag(1)-N(4)	107.84(10)	N(3A)-Ag(2)-N(3)	180.0	N(7)-Ag(3)-N(7A)	180.00(10)

[a] Symmetry transformations used to generate equivalent atoms: For **1**: A -x + 1/2, -y + 3/2, -z; For **2**: A -x+1,-y+1,-z+2; B-x+1,-y,-z+2. For **3**: A -x + 1/2, -y + 3/2, -z; For **4**: A -x+3,-y,-z+1, -z; For **5**: A x+1, y, z.

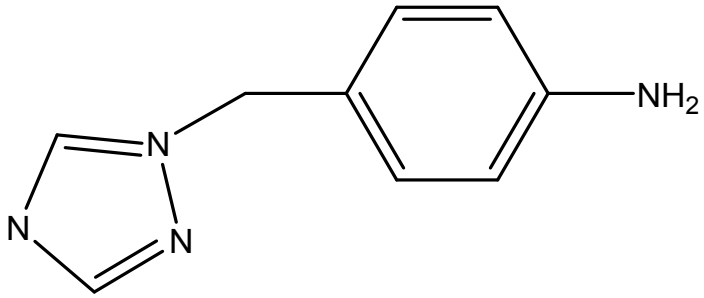

Scheme S1. A Schematic Presentation of the new versatile multi-dentate 1-(4-aminobenzyl)-1,2,4-triazole ligand.

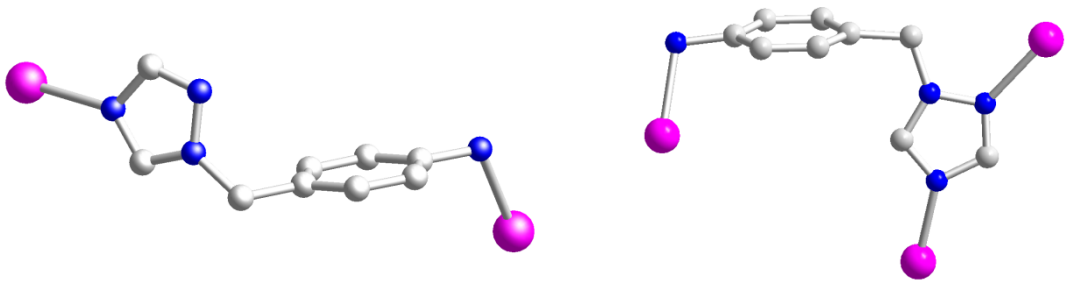

(a) (b)

Scheme S2 Two different bridging coordination modes of new abtz ligand (Color code: Purple, Metal; Blue, N; Light Grey, C).

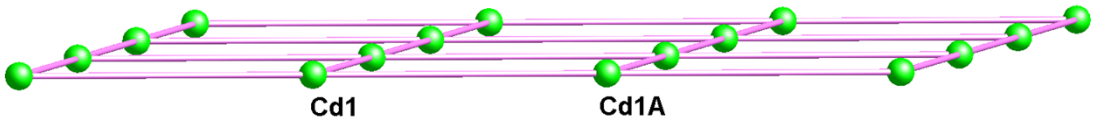

Fig. S1 All Cd^{II} ions in each layer in the 2D framework of **1** are strictly coplanar.

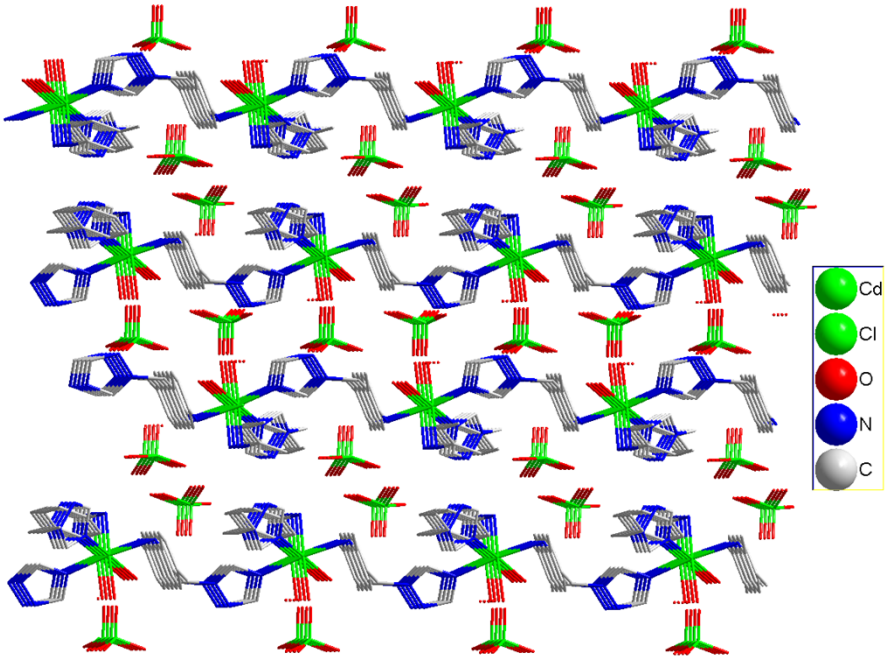

Fig. S2 2D coordination micro-porous framework of compound **1**, in which two kinds of different directional free perchlorate anions can be observed between two neighboring layers.

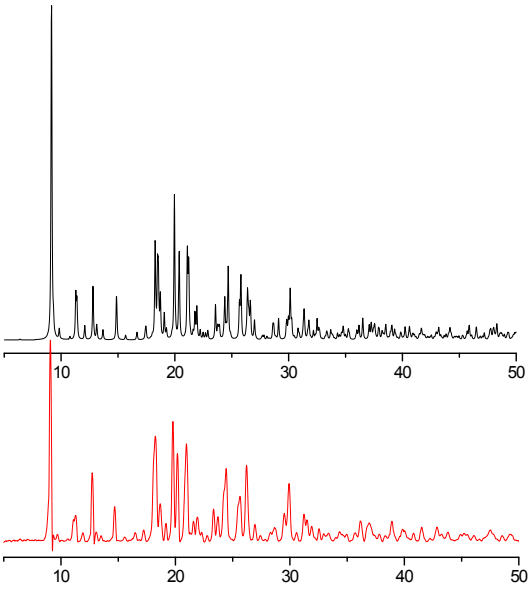

Fig. S3 Powder X-ray diffraction (PXRD) patterns of **1** (black for calculated and red for experimental ones).

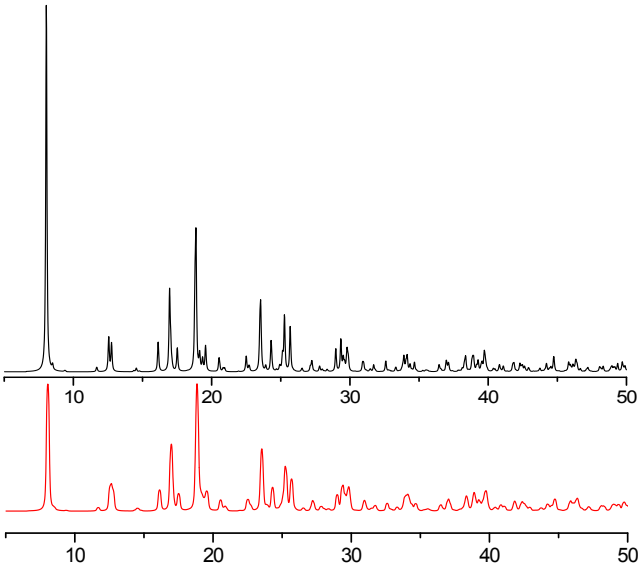

Fig. S4 Powder X-ray diffraction (PXRD) patterns of **2** (black for calculated and red for experimental ones).

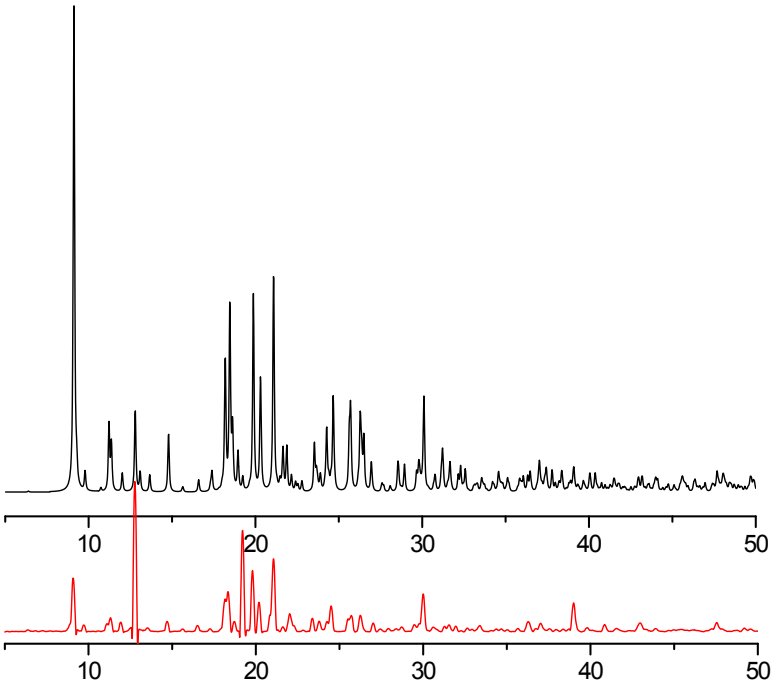

Fig. S5 Powder X-ray diffraction (PXRD) patterns of **3** (black for calculated and red for experimental ones).

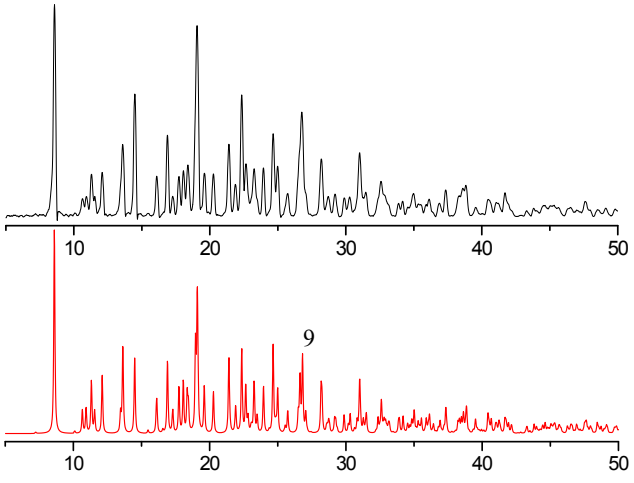

Fig. S6 Powder X-ray diffraction (PXRD) patterns of **4** (black for calculated and red for experimental ones).

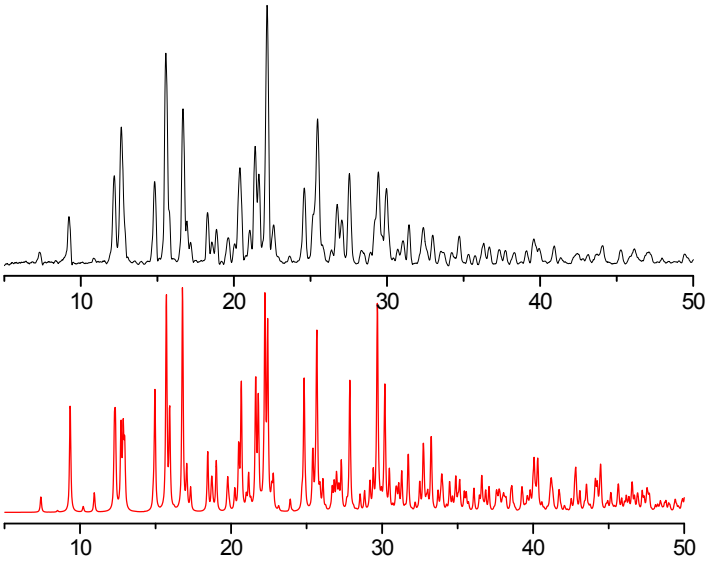

Fig. S7 Powder X-ray diffraction (PXRD) patterns of **5** (black for calculated and red for experimental ones).

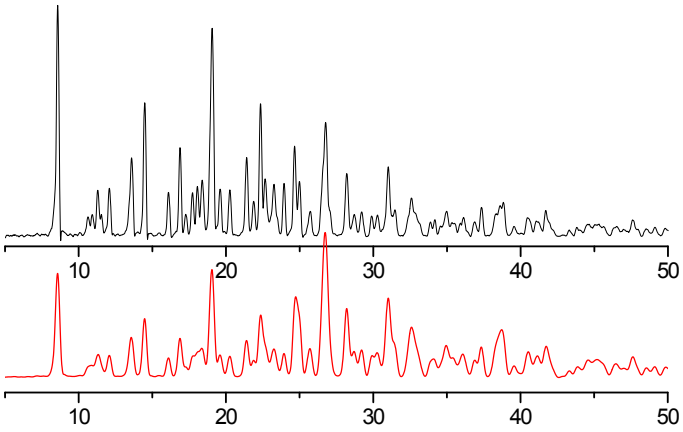

Fig. S8 Powder X-ray diffraction (PXRD) patterns of the used samples **4** before (black) and after (red) suspending in the analyte solution confirming the integrity of the frameworks.

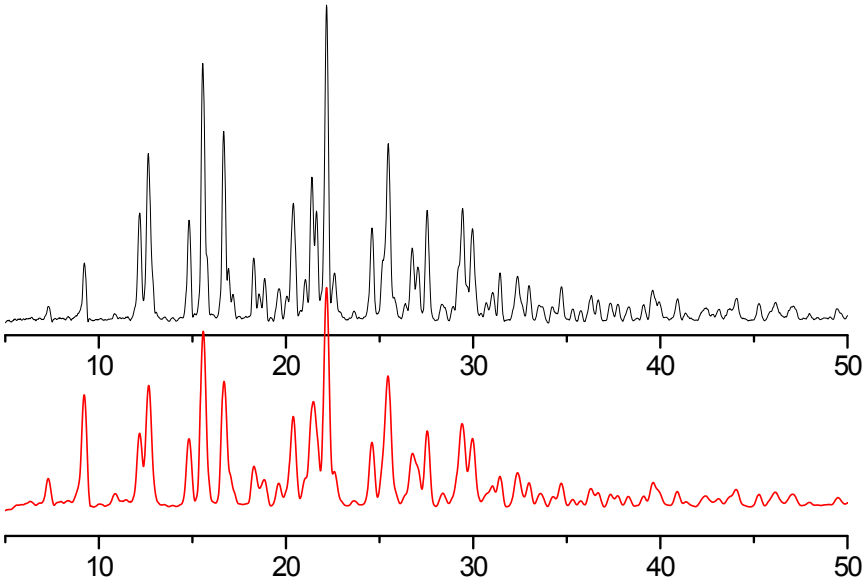

Fig. S9 Powder X-ray diffraction (PXRD) patterns of the used samples **5** before (black) and after (red) suspending in the analyte solution confirming the integrity of the frameworks.

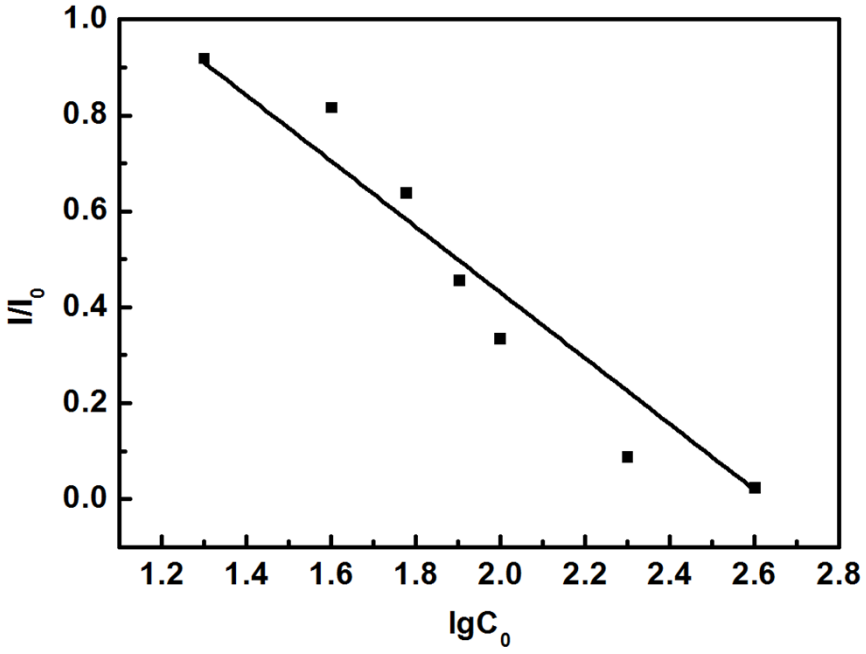

Fig. S10 The luminescent quenching effect of different concentrations of Fe^{3+} can be treated with the Stern-Volmer equation, $I_0/I = 1 + Ksv[Q]$, where Ksv is the quenching constant and [Q] is the quencher concentration.

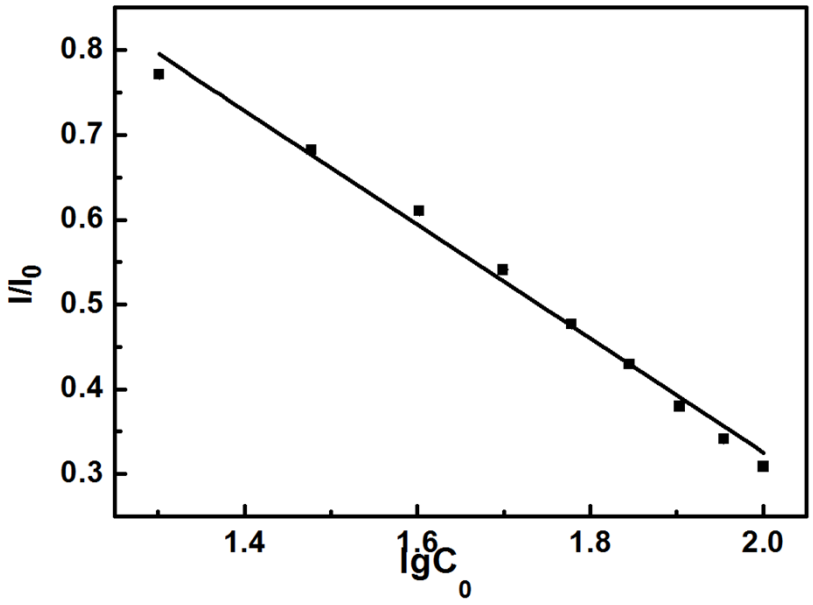

Fig. S11 The luminescent quenching effect of the different concentrations of actone into the water solutions can be treated with the Stern-Volmer equation, $I_0/I = 1 + Ksv[Q]$, where Ksv is the quenching constant and [Q] is the quencher concentration.

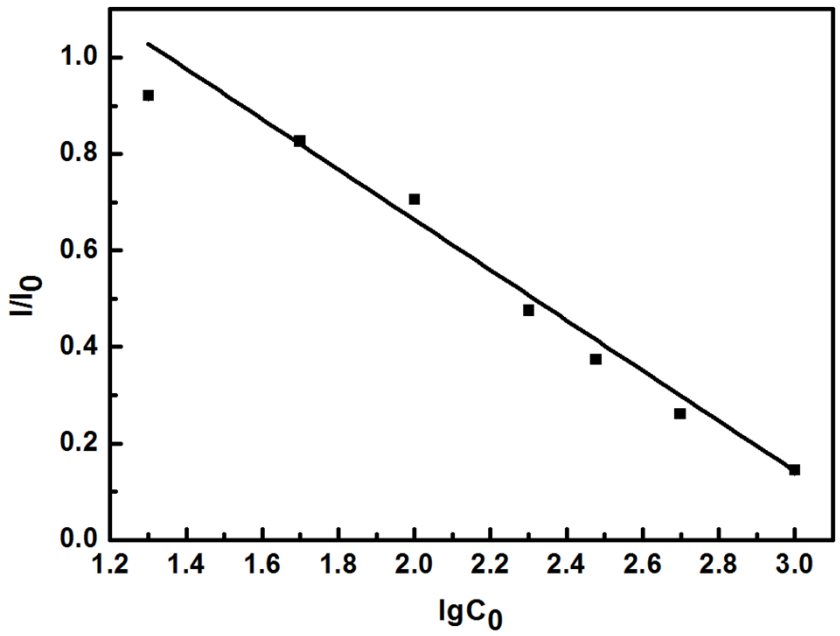

Fig. S12 The luminescent quenching effect of different concentrations of vitamin C in the water solutions can be treated with the Stern-Volmer equation, $I_0/I = 1 + Ksv[Q]$, where Ksv is the quenching constant and [Q] is the quencher concentration.